れてきました。そして、分子系統的な確証はありませんが、これらを合せて、クロミスタ(Chromista)という分類群をつくるという仮説が提唱されています[10]。

そして、いずれも紅藻由来の葉緑体を持つ藻類を含むクロミスタとアルベオラータを更に合せて、クロムアルベオラータ(Chromalveolata, Fig. 28)というスーパーグループを作るという仮説が提唱されています[21. Cavalier-Smith 1999]。クロムアルベオラータ仮説は、全ての共通祖先の時代に、同一の紅藻を二次共生させて、繊毛虫や無色ストラメノパイルは後天的に二次共生葉緑体を喪失したということを主張します。つまり、真核生物における紅藻由来の葉緑体は、全て同一起源であると提案しているものですが、あくまで仮説で決定的証拠はありません。実際、クリプト藻とハプト藻は、有中心粒太陽虫などの原生動物と独立した大系統群ハクロビアを作る[11]などとも言われており、覆る可能性も十分にはらむ仮説です。この先、この分類群にどう決着が着くかまだまだわかりません。

進化の大部屋・原生生物の世界

多様な藻類の世界は、広大に分岐多様化した原生動物の世界へ、緑藻や紅藻が多発的に飛び込んで創出されました。クロララクニオ藻やユーグレナ藻のように原生動物時代の姿を色濃く残すものや、不等毛藻のように藻類としての生き方を極め、独自に多様化していったものまでさまざまです。また、アピコンプレクサや渦鞭毛虫、卵菌、もしかしたら繊毛虫のように、かつては藻類として生きていたのに、原生動物としての生き方に戻ったとされるものまでいます。

藻類とは何でしょうか。この問いかけは、同時に原生動物とは何か、という問いかけにもなるでしょう。動物と植物の関係のように、原生動物と藻類をきっちりと区別しようとすることもあります。しかし、藻類の多様性を理解すると、藻類と原生動物は複雑に入り混じった存在で、単純に区別できるわけではなさそうです。

生物の進化の中で、真核藻類は、原生動物から分岐して創出されてきました。そういう意味で、藻類と原生動物は、互いに「進化の隣人」であると言えます。

ところが、話は更に複雑で、葉緑体を獲得して藻類になったものが、再び原生動物の生き方に戻るという葉緑体の退化・喪失という現象も見られます。

そうなると、もはや完全に区別できるような隣人の関係ではなく、むしろ、“大きな部屋”の中で“ふらふら”しながら共存しているような「進化の大部屋の住人たち」と言えるかもしれません。

この「大部屋」には、きちんと名前がついています。かつてヘッケルが命名し[22. Haeckel 1866]、ホイタッカーが採用して[23. Whittaker 1969]、マーグリスが洗練させた[24. Margulis 1970]、「原生生物」という名称です。原生生物(Protist)は、原生動物と藻類という存在を考える上で、とても優れた概念です。原生生物は、マーグリスによって、動物・植物・真菌以外の真核生物の補集合として定義されましたが、言いかえれば、原生動物と藻類、その他、卵菌やラビリンチュラなど菌様生活をしている全ての真核生物の総称であると言えます。これらの生物は、互いに完全に線引きのできない仲間たちであることは、ここまで読んで頂いた皆さんなら理解できるはずです。

原生生物の世界。原生動物と藻類、更に菌様生物たちが、ごちゃ混ぜになった進化の大部屋です。

原生動物と藻類の生き方(*)

近年の生物分類は、分岐進化に即した単系統性を重要視する系統分類が主流です。しかし、原生動物と藻類は、いわゆる多系統的な、しかも互いに区別することのできない存在です。原生動物や藻類は、系統を重視した名前ではなく、むしろ生き方を表していると言えるでしょう。すなわち、

原生動物
捕食や運動といった動物的生活をしている単細胞の真核生物

藻類
光合成によって生活している生物

原生動物や藻類とは、あくまで生き方を表した名前というわけです。しかも、この生き方は必ずしも両立できないものではありません。これまで紹介してきた藻類の大半は、運動性を持って立派に原生動物の生き方をしてますし、黄金色藻や渦鞭毛藻のように捕食を行うものもいました。彼らは藻類であると同時に原生動物なんですね。日本語と同時に英語も使えるような、バイリンガルみたいなものでしょうか。

更に、一見すると完全に原生動物のような存在も、昔は葉緑体を持っていたものが多くいることを踏まえると、彼らもまた、大きな枠組みの中では、藻類と呼んでもいいのかもしれません。

---

*) 原生動物と藻類、更に原生生物の定義については、統一的な意見はなく、研究者によって違っている(下に例を列挙)というのが現状です。したがって、この稿で述べていることも、あくまで一つの意見に過ぎないという事を理解ください。分類の話に正解は無く、そこが、研究の世界の多様性とも言えます。

例) 原生動物は、葉緑体を持たない従属栄養性の真核生物、藻類は、葉緑体を持つ独立栄養性の真核生物とする。
例) 藻類＝植物であり、不等毛植物、ユーグレナ植物などと呼ぶ。
例) 原生動物と原生生物は、同じ存在で、藻類は含めない。
例) 大型藻類は、原生生物に含めない。植物である。
例) シアノバクテリアは藻類に含めない、あるいは含める。
例) 陸上植物は藻類に含めない。あるいは含める。
例) 葉緑体を持たなくても、おなじ系統に葉緑体を持つものがいれば、藻類とする(渦鞭毛虫、卵菌、ラビリンチュラなど)

共生藻・奪葉緑体
Symbiotic algae and Kleptochloroplast

藻類とは、生き方の名前であると述べました。その概念を受け入れると、更に藻類の範囲は広がります。

サンゴ(Fig. 24)は皆さんご存知ですね。サンゴは、固着性の刺胞動物の仲間ですが、光合成に依存して生きています。サンゴに細胞内共生している褐虫藻と呼ばれる渦鞭毛藻(zooxanthella)から、光合成支援を受けているのです。褐虫藻は、他にもタコやシャコガイの仲間や、放散虫、有孔虫、繊毛虫といった原生動物にも細胞内共生をして、光合成支援をしています。

淡水環境では、さまざまな原生動物や無脊椎動物の細胞内で緑藻類の共生クロレラ(zoochlorella)を見ることができます(Fig. 25)。例えば、サンゴと同じく刺胞動物のヒドラには、グリーンヒドラと呼ばれる腸細胞に共生クロレラを持つものがいます。このグリーンヒドラ、筆者の研究室にもいるのですが、共生クロレラの光合成支援がある為か、強いです。数ヶ月、餌を与えなくても、光さえ与えておけば長生きします。

共生クロレラを持つ原生動物は、アメーバ、太陽虫、繊毛虫類と、多く見ることができ、有名どころの原生動物には必ずいるといってもいいくらいです。

zooxanthellaやzoochlorellaの仲間は、「共生藻」と呼ばれており、現在進行形の二次共生とされています。共生藻は、基本的に宿主の細胞内で分裂増殖をして、世代を超えて受け継がれる、擬似的な葉緑体として機能しています。

藻類から葉緑体を奪って利用する生物も知られています。無脊椎動物のウミウシの仲間には、ミルやフシナシミドロなどの藻体細胞から葉緑体を吸い取り、腸の細胞に共生させるものがいます。渦鞭毛藻の項で紹介したカンムリムシ(*Dinophysis acuminata*, Fig. 9)などの渦鞭毛虫や、繊毛虫(*Mesodinium rubrum*など, Fig. 26)、太陽虫といった捕食性原生動物の仲間にも、別の微細藻から葉緑体を奪って自分のものとして利用するものが知られています。別の藻類から奪った葉緑体は、「奪葉緑体」と呼ばれています。

共生藻や奪葉緑体を持つ生物は、捕食と光合成を同時に行う複合栄養生物ですが、写真を見てもらえばわかるように、細胞に葉緑体由来色がついていて、まるで藻類です。そして、実際に光合成に依存した藻類としての生き方をしています。そういう意味では、彼らも藻類の仲間かもしれません。

生物の世界は、このように何度も起こり、今も起こっている藻類の細胞内共生を通して、多様な光合成生物の世界を創り出し、創り出されているんですね。

この稿は、藻類として生活している、あるいは生活していた生物を、できる限り網羅的に紹介することを目指しました。それでも、紹介しきれていない藻類の仲間たちは、まだまだいます。未発見の子も多くいるでしょう。藻類という生き方、そして、彼らが生きているこの広い生物の世界の魅力を、より一層、感じられるようになったら嬉しく思います。

(文責・早川昌志)

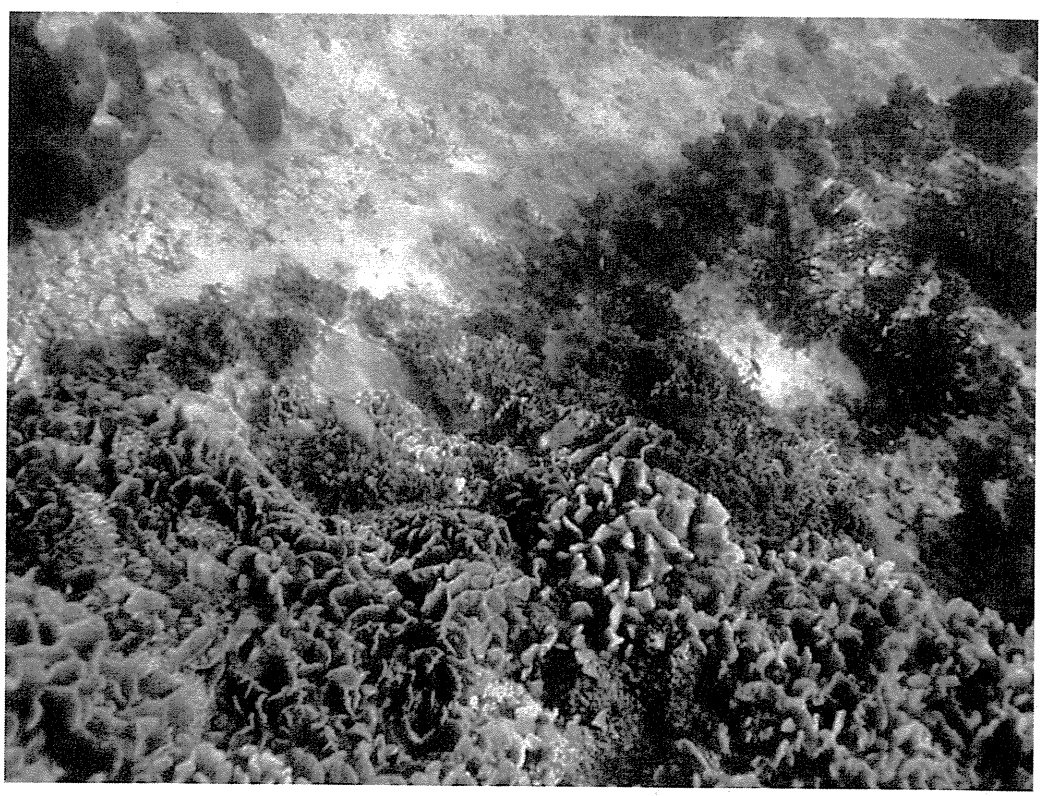

Fig. 24 サンゴ (西村文秀氏写真提供)

Fig. 25

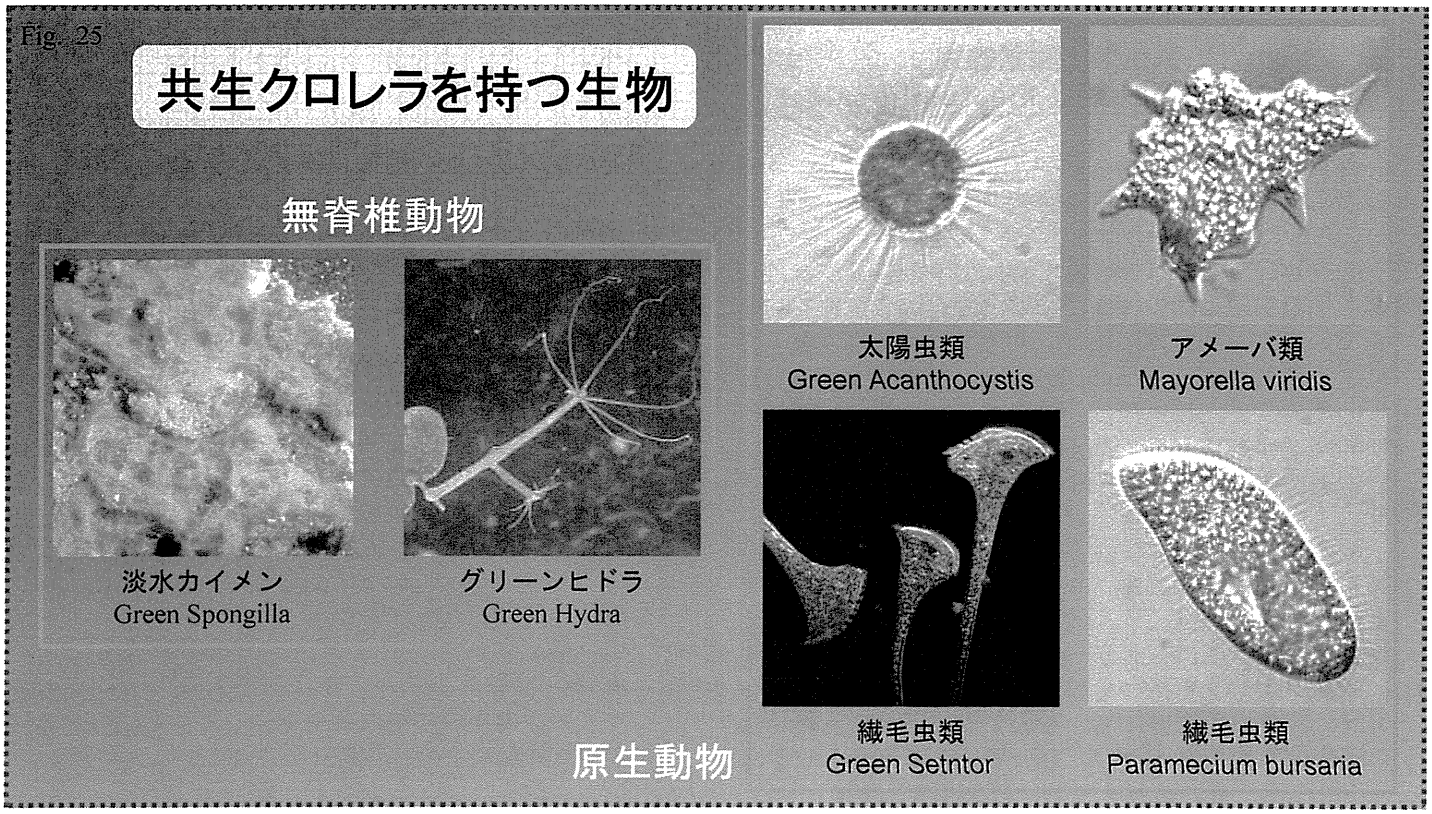

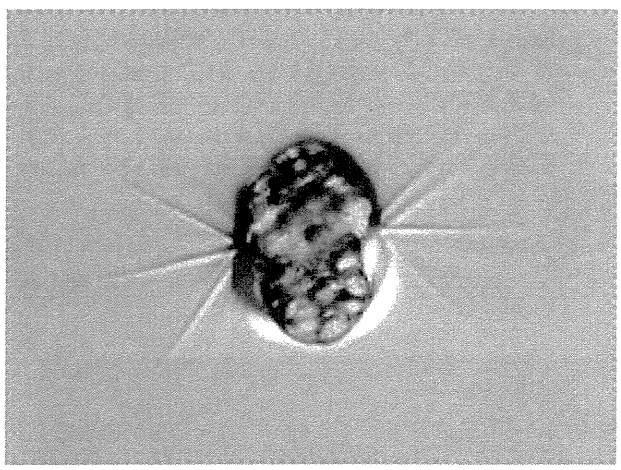

Fig. 26 *Mesodinium rubrum* (Myrionecta rubra)
海洋に生息する繊毛虫類の仲間。クリプト藻を起源とする奪葉緑体を持つ。（写真提供：末友靖隆博士・松山幸彦博士「日本の海産プランクトン図鑑」（共立出版）より）

Acknowledgment

「藻類の仲間たち」には、多くの研究者の方々に、美しい写真をご提供いただきました。この場を借りて、厚く御礼申し上げます。藻類、原生動物、そして原生生物の世界の魅力を、より多くの方々に知ってもらえる機会になることを祈ってます。

西村文秀氏（神戸大学） Fig. 1 (海藻の仲間たち)、Fig. 24 (サンゴ)
加藤将博士（神戸大学） Fig. 2 (シャジクモ)
金澤篤志氏(岡山大学) Fig. 10 (CoscinodiscusのSEM写真)
一宮睦雄講師（熊本県立大学）、桑田晃博士(東北区水産研究所)、山田和正氏(福井県立大学) Fig. 14 (パルマ藻)
永宗喜三郎室長、福士路花氏、海老根一生博士(国立感染症研究所) Fig. 20 (アピコンプレクサの仲間たち)
吉見英明氏(神戸大学) Fig. 21 (エキビョウキンの遊走子)

「日本の海産プランクトン図鑑」（共立出版 2011 岩国市立ミクロ生物館監修）より
写真撮影者：末友靖隆（岩国市立ミクロ生物館）・松山幸彦（(独)水産総合研究センター）
Fig. 9 (渦鞭毛虫・渦鞭毛藻の仲間たち・多数)、Fig. 12 (オオチャヒゲムシ)、Fig. 13 (ディクチオカ藻の仲間たち)、Fig. 26 (*Mesodinium rubrum*)

＊撮影者の記述のないものは、早川が撮影。

References.

[1] McCourt et al. (2004) Charophyte algae and land plant origins. TRENDS Ecol. Evol., 19: 661-666.
[2] Bhattacharya and Medlin (1995) The phylogeniy of plastids: A review based on comparisons of small-subunit ribosomal RNA coding regions. J. Phycol., 31: 489-498.
[3] Suzaki and Williamson (1986) Cell surface displacement during euglenoid movement and its computer simulation. Cell Motil. Cytoskeleton, 6: 186-192.
[4] Geitler (1930) Ein grünes Filarplasmodium und andere neue Protisten. Archiv für Protistenkunde, 69: 614-636.
[5] Fukuda and Endoh (2006) New details from the complete life cycle of the red-tide dinoflagellate Noctiluca scintillans (Ehrenberg) McCartney. Eur. J. Protozool, 42: 209-219
[6] Holwill and Patricia (1974) Dynamics of the hispid fllagelum of Ochromonas danica The role of Mastigonemes. J. Cell. Biol, 62: 322-328.
[7] Ichinomiya et al. (2011) Isolation and characterization of Parmales(Hetetokonta/Heterokontophyta/Stramenopiles) from the Oyashio region, western North Pacific. J. Phycol, 47: 144-151.
[8] McFadden (1990) Evidence that cryptomonad chloroplasts evolved from photosynthetic eukaryotic endosymbionts. J. Cell Sci., 95: 303-308.
[9] Sepsenwol (1973) Leucoplast of the cryptomonad Chilomonas paramecium. Exp. Cell Res., 76: 305-409
[10] Cavalier-Smith (1993) Kingdom protozoa and its 18 phyla. Microbiol. Mol. Biol. Rev., 57: 953-994.
[11] Okamoto et al. (2009) Molecular phylogeny and description of the novel Katablepharid Roombia truncata gen. et sp. nov., and establishment of the Hacrobia taxon nov. PLoS One, 4: e7080
[12] Margulis (1970) Origin of Eukaryotic Cells. (Yale University Press).
[13] Gibbs (1981) The chloroplasts of some algal groups may have evolved from endosymbiotic eukaryotic algae. Annals New York Acad. Sci., 361: 193-208.
[14] Cai et al. (2003) Apicoplast genome of the coccidian Eimeria tenella. Gene, 321: 39-46.
[15] Waller and McFadden (2005) The apicoplasst: a review of the derived plastid of apicomplexan parasites. Curr. Issues Mol. Biol., 7: 57-80.
[16] Lang (1963) Electron-microscopic demonstration of plastids in Polytoma. J. Eukaryot. Microbiol., 10: 333-339.
[17] Tyler et al. (2006) Phytophthora genome sequences uncover evolutionary origins and mechanisms of pathogenesis. Science, 313: 1261-1266.
[18] Moore et al. (2008) A photosynthetic alveolate closely related to apicomplexan parasites. Nature, 451: 959-963
[19] Horiguchi and Pienaar (2004) Ultrastructure of a new marine sand-dwelling dinoflagellate, Gymnodinium quadrilobatum sp. nov. (Dinophyceae) with special reference to its endosymbiotic alga. Eur. J. Phycol., 29: 237-245.
[20] Reyes-Prieto (2008) Multiple genes of apparent algal origin suggest ciliates may once have been photosynthetic. Curr. Biol., 18: 956-962.
[21] Cavalier-Smith (1999) Principles of protein and lipid targeting in secondary symbiogenesis: Euglenoid, Dinoflagellate, and Sporozoan plastid origins and the eukaryote family tree. J. Eukaryot. Microbiol., 46: 347-366.
[22] Hackel (1866) Generelle Morphologie der organismen. (Berlin).
[23] Whittacker (1969) New concepts of kingdoms of organisms. Science, 163: 150-160
[24] Margulis (1970) Whittaker's five kingdoms of organisms: minor revisions suggested by considerations of the origin of mitosis. Evolution, 25: 242-245.

その他参考文献
「日本の海産プランクトン図鑑」（共立出版 2011 岩国市立ミクロ生物館監修）
　「藻類の仲間たち」に登場する原生生物の和名の一部は、本書で創設されたものから引用しています。
「バイオダイバーシティ・シリーズ3 藻類の多様性と系統」（裳華房 1999 岩槻邦夫・馬渡峻輔監修）
「やさしい日本の淡水プランクトン図解ハンドブック」（合同出版 2005 若林徹哉監修）
「淡水微生物図鑑」（誠文堂新光社 2010 月井雄二 著）

Information.

「藻類の仲間たち」に登場する生物の分類は、必ずしも正しいことを保障するものではありません。あくまで参考程度に楽しんで頂くようお願いします。

Websites.

岩国市立ミクロ生物館ホームページ（http://www.shiokaze-kouen.net/micro/）
早川昌志(文責者)個人ホームページ（https://sites.google.com/site/symchlorosome/）

生水と原虫症(生水のリスク)

泉山 信司　八木田 健司　永宗 喜三郎

はじめに

飲料水を介して伝播する病原体は腸管感染性の細菌やウイルスがよく知られるところであるが，寄生虫学分野においてもクリプトスポリジウム，ジアルジア，赤痢アメーバなどの原虫類(真核単細胞生物の寄生虫)が知られている．従来は煮沸消毒により，近年はボトル水の利用が進んで生水の利用は回避されているが，それでもキャンプ場の水道施設や地域の小規模水道を介した感染事故は起きている．腸管感染性の病原体の感染経路は単純で，便に混じって排出された病原体により食品や水が汚染されることによる，いわゆる糞-口感染である．水の糞便汚染は直接的な感染源になるばかりでなく，間接的な食品汚染などにつながり，大きな事故に発展する．一方，山間部に降り注いだ雨が海に達するまでの間，取水・使用・排水が繰り返され，水は容易に糞便汚染を受ける．そのため，安全な飲料水の確保には，消毒やろ過といった水処理が必須となっている．

1848年に始まったロンドンのコレラの大流行においては，3万人が罹患して1万人以上が死亡した[1]．この事例では後に水道水の汚染が疑われ，1854年の再流行では水道を止めることで流行が収束している．この時の調査がいわゆる疫学の始まりとされる．一方，原虫症においても水の汚染の影響は大きく，1993年のミルウォーキーの水道水を介したクリプトスポリジウム症の水系集団発生では，感染者は40万人に及んだとされる[2]．わが国も例外ではなく，1996年に埼玉県越生町の水道水を介したクリプトスポリジウム症の水系集団感染で，地域住民の6割強の8,800人が発症したとされる[3]．

国内の水系感染に関する統計はないが，原虫に限らず，細菌・ウイルスを含む様々な水系集団感染が報告されている(**表1**)．細菌性水系感染事例の手集計によれば，過去15年間に少なくとも84件の飲料水起因の集団感染が発生し，井戸水がその内の5割，湧水・沢水では1割であった(**表2**)．少数の感染が見落とされて集団感染に偏った可能性は否定できないが，患者数は3万人以上に及び，生水や不適切な管理下の井戸水に感染症のリスクが指摘される．

原虫症の概要

水を介して糞口感染する可能性のある原虫類としては，クリプトスポリジウム，ジアルジア，赤痢アメーバなどが主要なものとして挙げられるが，海外ではそれらに加えて，ベリー類の汚染が問題となったサイクロスポラによる食中毒や水系感染，ネコの糞便汚染によるトキソプラズマの水系感染等が知られている[4,5]．

一般に原虫に感染すると，糞便中に多くの感染型のオーシスト(あるいはシスト；嚢子)が排出さ

いずみやま しんじ，やぎた けんじ，ながむね きさぶろう：国立感染症研究所寄生動物部
連絡先：〒162-8640 東京都新宿区戸山1-23-1

0368-5187/12/¥500/論文/JCOPY

表1　主な水系集団感染[1)]

発生年	場所	発症者数	病原体	原因等
1953	千葉県茂原市水道	7,000	ウイルス疑い(ろ過性病原体)	水道疑い，集水施設破損，消毒不備
1977	佐賀県基山町小学校	486	A型肝炎ウイルス	浄化槽の工事の問題で井戸水が汚染
1982	札幌市ストア	7,751	カンピロバクター	井戸の汚染
1990	浦和市幼稚園	319	腸管出血性大腸菌O157	浄化槽汚水により井戸水が汚染
1994	平塚市雑居ビル	461	クリプトスポリジウム(*C. parvum* ウシ型)	ビル受水槽が下水により汚染
1996	埼玉県越生町水道	8,812	クリプトスポリジウム(*C. hominis*)	下水排水を下流で取水による循環
1998	長崎県　大学	821	赤痢菌(*S. sonnei*)	井戸の汚染
2002	北海道　宿泊施設	317	クリプトスポリジウム(*C. hominis*)	原因不明(水系感染が疑われた)
2004	長野県　宿泊施設	288	クリプトスポリジウム(*C. hominis*)	プール，蛇口の汚染
2005	秋田県　簡易水道	29	ノロウイルス	原水の汚染

出典：文献[1)]「水道の病原微生物対策　序章」より抜粋，他

表2　水源別，細菌性集団感染発生動向(1982～1996年)[1)]

飲料水の水源	発生件数	割合(%)
上水道	5	6.0
簡易水道	5	6.0
簡易専用水道	5	6.0
専用水道(表流水)	1	1.2
井戸水(専用水道および個人用)	45	53.6
湧水・沢水	10	11.9
その他(不明を含む)	13	15.5
合計	84	100

出典：文献[1)]「水道の病原微生物対策　3章」より抜粋

れるが，わずかな量の糞便による水の汚染で，すなわち少ない原虫数で感染が成立すること，さらに原虫自体が小さく除去困難であることで，水系感染は大規模になりやすい．汚染された水は，さらに食物を汚染したり，噴水や水泳プールといった親水施設等を介して水系感染する恐れもある．加えて，乳幼児のオムツ替えや動物との触れ合いといった患者・患畜との直接の接触感染があり，性感染症にもなる．

原虫類のオーシストあるいはシストは強い環境耐性があり，一般的な塩素消毒の効果は期待できないが，加熱，オゾン処理，紫外線・放射線により不活化され，また乾燥や凍結には弱い．適切なろ過により物理的な除去も可能である．

感染症法では，クリプトスポリジウム，ジアルジア，赤痢アメーバ症が5類の全数把握疾患に指定されている．しかし，患者からの積極的な検出は行われておらず，国内の生水・生食と原虫症の関係は明らかではない．これとは別に，水道におけるクリプトスポリジウム等検査法が整備され，水道原水の河川水等の汚染状況が把握されている(健水発第0330006号，平成19年3月30日，厚生労働省健康局水道課長通知)．加えて，飲食物を介した感染経路が考慮され，食中毒事件票における食中毒病因物質の分類『その他』の欄には，「クリプトスポリジウム，サイクロスポラ，アニサキス等」と例示されている(平成11年12月28日付衛食第166号，衛乳第248号，衛化第66号，厚生省生活衛生局食品保健課長，乳肉衛生課長，食品化学課長通知)．

クリプトスポリジウムについて

クリプトスポリジウムは，胞子虫類に属する原虫で，宿主の腸管上皮の微絨毛に虫嚢を形成する．寄生後，有性生殖により感染型のオーシストを産生し，糞便中にオーシストが排出される．オーシストは4～6 μm の球状で，中に4個のスポロゾイトと，残体などの顆粒が観察される．

国内では水道水や水泳プールを介した集団感染，海外ではそれらに加えて噴水などの親水施設での集団感染が報告されている．その他，サラダ，生牛乳や，落下リンゴのサイダーでの感染が報告されている[4)]．

クリプトスポリジウム症は非血性の水様下痢を

表3　クリプトスポリジウム症，ジアルジア症の国別の報告数（2006年度）[7]

国別	クリプトスポリジウム症		ジアルジア症	
	報告数	（対10万人）	報告数	（対10万人）
United States	6,071	2.05	18,953	7.28
United Kingdom	3,678	6.26	2,945	5.01
Germany	1,204	1.46	3,661	4.45
New Zealand	736	17.80	1,214	11.80
Canada	728	2.30	3,661	4.45
Belgium	402	3.80	1,238	11.80
Ireland	367	8.70	65	1.53
Spain	262	0.64	897	2.20
Sweden	103	1.13	1,277	14.01
Finland	6	0.11	272	5.18
日本	18	0.01	86	0.07

出典：文献[7]より抜粋

主徴とし，腹痛，吐き気，嘔吐，中程度の発熱などの症状を呈する．国内の集団感染事例における潜伏期間は6日（4～8日）で，通常1～2週間で症状は改善する．わずか1オーシストの摂取で4～16%の感染確率があるとされる．本症の特効薬は知られておらず，健常者においては脱水に対する対症療法が基本である[6]．自然治癒が期待できない免疫不全者においては，原疾患の治療が最善の方法であり，AIDS（後天性免疫不全症候群）におけるHAART（Highly Active Anti-Retroviral Therapy）や先天性免疫不全における骨髄移植等による免疫機能の回復が症状の改善に効果的である．ニタゾキサニド，パロモマイシン，アジスロマイシンが使われることもある．

クリプトスポリジウム属の宿主域は広く，哺乳類や鳥類，あるいは爬虫類や魚類にまで寄生が知られている．遺伝子解析の結果から，ヒトに強い親和性を持つ遺伝子型（*Cryptosporidium hominis*，あるいは*C. parvum* genotype I，あるいはヒト型）と，ヒトを含め広く哺乳類に親和性を示す遺伝子型（*C. parvum*，あるいは*C. parvum* genotype II，あるいはウシ型）が明らかにされている．国内では，*C. hominis*，*C. parvum*，*C. meleagridis*（トリ型）の順に感染事例が多く，従来心配されていた家畜由来の感染より，むしろヒト-ヒト感染の重要性が指摘される．

感染症法に基づく発生動向調査によると，年間の報告数はわずか10例前後で，海外の工業先進国との比較では，人口あたりの頻度がわが国では2桁も低い（**表3**）[7]．この結果がわが国の実態を端的に示しているかは疑問で，むしろ国内の検査体制の充実が求められていると解釈すべきではなかろうか．ちなみに，平成20（2008）年度の結果を中心とした水道の原水検査の結果では，209水道事業体中21事業体（約10%）において，クリプトスポリジウム，および後述のジアルジアが検出されており[8]，わが国においても確実に汚染が存在していることを示している．

ジアルジアについて

ジアルジア症はランブル鞭毛虫［*Giardia lamblia*（*syn. G. intestinalis, G. duodenalis*）］の感染により発症する．ジアルジアは鞭毛虫類に属し，栄養体は4対8本の鞭毛を有する．生活史は単純で，栄養体とシストからなり，栄養体の二分裂により増殖する．十二指腸，空腸上部に栄養体が寄生し，シストが糞便中に排出される．シストは5～8×8～12 μmの楕球形で，4つの核，曲刺，軸糸，鞭毛などが観察される．

強い下痢では環境耐性のないシスト化前の栄養体が多く排出されることがあり，下痢が治まってからの有形便中に無症候性に持続的にシストが排出されると，むしろ感染源としてのリスクが高まる．

ジアルジア症は下痢や腹痛，食欲不振，悪心，腹部不快感，鼓腸などで，下痢は非血性泥状便や粘性便から水様便，悪臭を放つ脂肪便が観察される．寄生が胆管や胆嚢にまで及ぶと，胆嚢炎様症状が見られることがある．潜伏期間は3～25日，平均7日とされる．本症には有効な治療薬として，国内ではメトロニダゾールが第一選択薬として頻用される．

ジアルジアはヒトの他にイヌ，ネコ，ウシ，ブタ，シカ，ウサギ，ビーバーやマスクラットなど広範囲の哺乳類に寄生する．複数の遺伝子型

(Assemblage)に分けられるが，ヒト由来の分離株は Assemblage A と Assemblage B に限られる．発生動向調査によると，年間の報告数はわずか 100 例弱で，海外の工業先進国との比較では人口あたりの頻度が，わが国では 2 桁も低い(**表 3**)．国内の実態や検査体制の解釈については，クリプトスポリジウムと同様に注意を要する．国内では戦後の混乱期にジアルジア感染が多数見られたと聞くが，集団感染事例の報告はない．

赤痢アメーバについて

赤痢アメーバ(*Entamoeaba histoliytica*)はアメーバ性赤痢の病原体であり，有症者の 80% 以上に腸管内の病変があり，病巣は壺形(あるいはフラスコ型)のアメーバ性潰瘍を呈する．腸アメーバ症では，腹部痙攣，軽度の腹痛，および血性・粘液性のイチゴゼリー状の便を呈する．赤痢アメーバ感染者の大半(85～95%)は不顕性感染で，感染者のおよそ 10% が有症となる．致死率の高い劇症型大腸炎や，肝臓，肺，脳に膿瘍を形成する腸管外アメーバ症も見られる．腸管アメーバ症，腸管外アメーバ症のいずれも，治療薬としてメトロニダゾール等が使用される．慢性に経過する例もあれば，肝膿瘍破裂など致命的な例もあり，重症例・劇症型で緊急手術となる．

赤痢アメーバは人獣共通感染症とされるが，ヒトが主要な保虫宿主である．疫学的には無症状シスト保有者の存在が重要で，食品加工に従事する者の健康管理には十分な配慮が求められる．熱帯から亜熱帯の衛生状態の悪い地域で多くの患者が見られ，一説には世界人口の 1 割が感染していると推定されている．発生動向調査によると，年間の報告数は 1,000 例程で，男性同性愛者間での感染，知的障害者施設での感染が知られている．海外ではシストに汚染された飲食物の摂取が感染経路となる一方，先進工業国では性感染症としての注意が求められている．潜伏期間は通常 2～4 週間とされるが，感染時期が不明な場合が多い．

生活史は単純で，栄養体とシストからなり，栄養体の二分裂により増殖する．栄養体は直径 10～50 μm で運動性に富み，赤血球を貪食した像が観察される．シストは直径 10～20 μm の球状で，内部に 4 つの核と類染色質体などが観察される．赤痢アメーバと非病原性アメーバ(*E. dispar*)は形態による鑑別ができず(*E. histolytica/E. dispar* と報告する)，原則として健常者から検出された *E. histolytica/E. dispar* は治療対象とならない．鑑別診断の方法には *E. histolytica* に特異的な PCR (polymerase chain reaction)，ELISA (enzyme linked immunosorbent assay)が用いられる．

おわりに

生水は各種病原微生物に汚染されている恐れがあり，生水の摂取は避けたい．その上，原虫には消毒抵抗性があり，原虫汚染の可能性のある水をろ過せずに，消毒のみ，かつ非加熱で使用する場合は感染のリスクが高い．生水リスクの管理には，患者試料からの検査を充実させ，国内における原虫症の感染の実態を明らかにし，もって公衆衛生をより向上させることが求められる．

文　献

1) 金子光美(編著)：水道の病原微生物対策．丸善，2006
2) Mac Kenzie WR, et al: A massive outbreak in Milwaukee of cryptosporidium infection transmitted through the public water supply. N Engl J Med **331**: 161-167, 1994
3) 埼玉県衛生部：「クリプトスポリジウムによる集団下痢症」―越生町集団下痢症発生事件―報告書(平成 9 年 3 月)，1997
4) 食中毒予防必携第二版．日本食品衛生協会，2007
5) WHO: Guidelines for Drinking Water Quality. Volume 1, 3rd (ed), 2004
6) 寄生虫症薬物治療の手引き　改訂第 7 版，ヒューマンサイエンス振興財団政策創薬総合研究事業「輸入熱帯病・寄生虫症に対する稀少疾病治療薬を用いた最適な治療法による医療対応の確立に関する研究」班，2010
7) 八木田健司，他：国内外におけるクリプトスポリジウム症ならびにジアルジア症の発生動向の現状と比較．第 68 回日本寄生虫学会東日本支部大会，2008
8) 松井佳彦，他：飲料水の水質リスク管理に関する統合的研究―微生物分科会．厚生労働科学研究費補助金(健康安全・危機管理対策総合研究事業)「飲料水の水質リスク管理に関する統合的研究」より平成 22 年度分担研究報告書，2011

A New Glucose-6-phosphate Dehydrogenase Deficiency Variant, G6PD Mizushima, Showing Increases in Serum Ferritin and Cytosol Leucine Aminopeptidase Levels

Yosuke Suga, Akira Nagita,* Rintaro Takesako,* Isao Tanaka,* Kaichiro Kobayashi,* Makoto Hirai,† and Hiroyuki Matsuoka†*

Summary: We made a diagnosis of glucose-6-phosphate dehydrogenase (G6PD) deficiency with a new mutation of 848A→G (exon 8) in a 16-year-old male patient presenting with severe hemolysis. He was administered a diclofenac sodium suppository (50 mg) at the time of first visit to our hospital because of pyrexia. In the acute phase, pyrexia, severe general fatigue, lumbar back pain, hemoglobinuria, and jaundice developed. Laboratory blood examinations showed hemolysis, and remarkable increases in serum ferritin and cytosol leucine aminopeptidase levels. Serum interleukin-6 and interferon-γ levels were also increased. No liver injury was found. He had neonatal jaundice persisting over 3 weeks. He did not have a history of chronic hemolysis or hyperbilirubinemia. Increases in serum ferritin or cytosol leucine aminopeptidase levels in G6PD-deficient patients were not reported earlier. In this case, it is presumed that infection and administration of anti-inflammatory agents induce the hemolytic episode and that hypercytokinemia deteriorates the disease condition.

Key Words: G6PD, G6PD deficiency, hemolysis, ferritin, cytosol leucine aminopeptidase, new mutation, hypercytokinemia, interleukin-6, interferon-γ

(*J Pediatr Hematol Oncol* 2011;33:15–17)

Glucose-6-phosphate dehydrogenase (G6PD) deficiency is the most common of the intraerythrocytic enzyme deficiencies, and about 140 genotypes have been described. New variant cases, however, are still found.[1] Compared with malaria endemic areas, the incidence of G6PD deficiency is very low (< 0.5%) in Japan.[2] Among such cases, 11 G6PD variants were found sporadically.[3–9] We encountered a G6PD-deficient patient with a new genome mutation. He developed acute hemolysis and remarkable increases in serum ferritin concentration and cytosol leucine aminopeptidase (LAP) activity after pyrexia. No G6PD-deficient patients with increases in serum ferritin and cytosol LAP levels were reported earlier. Herein, we describe a new genome mutation of G6PD and its clinical features.

CASE

A patient was a 16-year-old boy. He visited our hospital because of fever of 39°C in the afternoon of March 11, 2007. He was observed as an outpatient after administration of a diclofenac sodium suppository (50 mg) because no remarkably abnormal findings were found. He was admitted to our hospital the next day because of development of general fatigue, lumbar back pain, and a poor appetite as well. At the time of hospitalization, he was alert and had body temperature of 39.8°C, blood pressure of 110/50 mm Hg, regular pulsation, and heart rate of 90/min. There were no abnormal physical findings except icteric bulbar conjunctiva. Laboratory blood examinations showed high serum levels of total bilirubin (T-Bil) and C-reactive protein at 4.8 mg/dL and 3.321 mg/dL, respectively. No other abnormal findings were observed in the blood examinations (Table 1). An influenza antigen test was negative. Chest x-ray film showed no abnormal findings.

He had neonatal jaundice which persisted over 3 weeks and was resolved without any treatment. The maximum serum T-Bil level was 16.4 mg/dL on the 13th day after birth. He has had bronchial asthma from 1 year and 3 months of age. At the age of 9 years and 11 months, he was hospitalized because of high fever, general fatigue, and a poor appetite after administration of mefenamic acid and diclofenac sodium. At that time, hyperbilirubinemia (T-Bil: 3.6 mg/dL) was recorded. Although there were several occasions in which he was administered such agents, similar episodes did not occur then. He had no history of blood transfusion.

CLINICAL COURSE DURING HOSPITALIZATION

Although intravenous antibiotics (cefotiam) and oral acetaminophen were administered after admission, pyrexia, severe general fatigue, lumbar back pain, and poor appetite persisted. Hemoglobinuria and mild progression of anemia were found on the second hospital day, and serum aspartate aminotransferase, lactate dehydrogenase, and indirect bilirubin levels were increased, suggesting intravascular hemolysis. Serum ferritin concentration and cytosol LAP activity (Ono Pharmaceutical Co Ltd, Osaka, Japan) were also remarkably increased. On the second day, serum levels of interleukin-6 (38.7 pg/mL) and interferon-γ (6.4 IU/mL) were increased, although serum levels of interleukin-1β (< 10 pg/mL) and tumor necrosis factor α (2.2 pg/mL) were normal. The morphology of peripheral blood erythrocytes and the ultrasound examination of kidneys showed normal. Direct and indirect Coombs tests were both negative. Serum haptoglobin concentration (< 10 mg/dL) was decreased.

As drug-induced allergy or G6PD deficiency was suspected based on the above findings, all medications were discontinued in the evening of the second hospital day. The fever reduced gradually, and was free on the fourth day. Most marked findings indicating intravascular hemolysis were found on the third and fourth days. Plasma fibrinogen and fibrinogen degradation products levels were 422 mg/dL and 36.5 μg/mL, respectively, on the third day. Serum blood urea nitrogen and creatinine concentrations were the highest on the third day, whereas serum

Received for publication December 29, 2009; accepted August 2, 2010.
From the *Department of Pediatrics, Mizushima Central Hospital; and †Department of Infection and Immunity, Division of Medical Zoology, Jichi Medical University, Japan.
Reprints: Yosuke Suga, Department of Pediatrics, Mizushima Central Hospital, 4-5, Aoba-cho, Mizushima, Kurashiki-shi, Okayama, Japan (e-mail: jm-y.suga@kochi-u.ac.jp).

TABLE 1. Laboratory Data

	March 12	March 13	March 14	March 15	Convalescent Phase	Reference Value
WBC (/μl)	3900	6100	4600	5300	7600	3000-8900
RBC ($\times 10^4$/μL)	381	354	323	296	399	420-550
Hemoglobin (g/dL)	13.2	12.3	11.1	10.3	13.7	13.5-17.0
Platelet ($\times 10^4$/μL)	16.2	13.2	10.9	12.5	29.9	12.0-39.0
CRP (mg/dL)	3.3	6.5	7.6	3.9	0.3	< 0.40
AST (IU/L)	36	71	95	96	13	10-35
ALT (IU/L)	16	17	18	36	9	7-42
γ-GTP (IU/L)	19	20	19	20	16	5-60
LDH (IU/L)	239	638	1282	1339	152	120-240
Total Bil (mg/dL)	4.8	5.7	5.6	4.2	0.9	0.2-1.0
Direct Bil (mg/dL)	ND	0.7	0.2	ND	0.2	< 0.3
Indirect Bil (mg/dL)	ND	5.0	5.4	ND	0.7	
BUN (mg/dL)	11.1	12.3	15.3	13.4	13.0	8-20
Creatinine (mg/dL)	0.88	0.89	0.91	0.81	0.84	0.60-1.10
Uric acid (mg/dL)	6.2	ND	4.2	3.9	7.3	3.5-7.5
Ferritin (ng/mL)	ND	1457	1443	ND	224	22.5-233.0
C-LAP (IU/L)	ND	393	428	348	25	< 35

γ-GTP indicates γ-glutamyl transpeptidase; ALT, alanine aminotransferase; AST, aspartate aminotransferase; Bil, bilirubin; BUN, blood urea nitrogen; C-LAP, cytosol leucine aminopeptidase; CRP, C-reactive protein; LDH, lactate dehydrogenase; ND, not done; RBC, red blood cells; WBC, white blood cells.

uric acid concentration was the lowest on the fourth day. General fatigue and back pain disappeared as pyrexia resolved.

We measured G6PD activity of the patient's erythrocytes according to the WST-8/1-methoxy phenazine methosulfate method.[10] The G6PD activity was decreased to less than 10% of that of the wild type. Furthermore, we performed genetic analysis, which revealed that he had a point mutation (cDNA848A→G) in exon 8. Amino acid substitution would be 183 Asp to Gly. His family members also underwent the measurements of G6PD activity and the genetic analyses. They showed that his younger sister, mother, and mother's mother were gene carriers, and that their enzymatic activities were 90%, 50%, and 50%, respectively (Fig. 1). There are no relatives from overseas regarding the past 3 generations.

DISCUSSION

The patient's genome mutation site has not been reported earlier and there are no relatives from overseas in his ancestry, suggesting that this mutation does not originate from a common ancestor but is sporadic. We wish to nominate the new mutation as G6PD Mizushima. The World Health Organization classified the mutation of G6PD into class I to V depending on the enzyme activity and symptoms.[1,2] The patient's G6PD activity was lower than 10%, and he presented with an acute hemolytic episode. On the basis of these findings, he was classified as class II. Clinical symptoms of class II are general fatigue, anemia, and jaundice in the acute phase,[1,2] which are compatible with the patient's clinical findings. A cluster of mutations in exons 10 and 11 has been reported to cause a severe phenotype (class I, chronic nonspherocytic hemolytic anemia).[1] As the patient's mutation site was away from exons 10 and 11, it is probably why his symptoms were milder than those of class I.[1] His younger sister's G6PD activity was 90%, although she was gene carrier. In the field conditions, we sometimes encounter a young woman with heterozygous G6PD variant who shows nearly a normal level of the enzyme activity. With WST-8 test kits, we are regretful to describe that it is difficult to distinguish young women to be G6PD heterozygous or to be wild types.

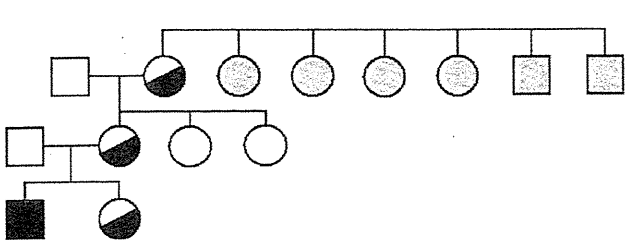

FIGURE 1. Family tree of the case.

Mild increases in serum ferritin concentration in G6PD-deficient patients were reported.[11] The increases were presumed to be because of both shortened life-span and increased break down of erythrocytes, or to be caused in increased storage iron attributed to blood transfusion.[11] Increases in serum ferritin concentration were mild in patients with sickle cell crisis who did not undergo blood transfusion.[12] Moreover, increases in serum ferritin concentration are considered in liver injury, hemochromatosis, inflammatory syndromes, cytolysis, Still disease, and hemophagocytic syndrome.[13,14] He had no history of blood transfusion. Serum ferritin concentration was within the normal range in the convalescent phase and was remarkably increased in the acute phase. Serum alanine aminotransferase activity was normal in the present acute phase. Ferritin is induced by some cytokines,[15] and its serum concentration is remarkably elevated in hypercytokinemia.[16] Serum levels of interleukin-6 and interferon-γ were increased. These suggest that the remarkable increase in serum ferritin concentration is because of hypercytokinemia.

LAP is classified as cytosol and microsome. It is considered that serum cytosol and microsome LAP activities increase in liver injury and biliary disorders, respectively.[17] Cytosol LAP assay kit used in this case used L-leucinamide as a substrate, which is predominantly catalyzed by cytosol

LAP. High cytosol LAP activity is found in lymphocytes and many other organs as compared with erythrocytes.[18] An earlier report showed that increases in serum cytosol LAP activity were found in patients with measles and rubella.[19] We have treated several cases of hemophagocytic syndrome showing remarkable increases in serum cytosol LAP activity and ferritin concentration (unpublished data). Cytosol LAP is induced by some cytokines.[20] Although hypercytokinemia is thought to disorder various tissues, neither liver injury nor biliary disorders were found in this acute phase. Remarkable increases in serum cytosol LAP activity were found in the acute phase but not in other hemolytic disorders such as hemolytic uremic syndrome and spherocytic anemia. Serum levels of interleukin-6 and interferon-γ were increased in this case. On the basis of these results, we presume that abundant cytosol LAP was induced in activated tissues under hypercytokinemia and released into blood stream during erythrophagocytic process. This pathologic state would be the results in a remarkable increase in serum cytosol LAP activity.

The hemolytic attack in G6PD-deficient patients is thought to be developed with oxidant stress triggered by infection.[1] Uric acid has an antioxidant effect. Serum uric acid concentration was decreased as compared with serum urea and creatinine concentrations in the acute phase, suggesting that oxidant stress was also increased in this patient. Erythrocytes exposed oxidant stress are developed not only intravascular hemolysis but also erythrophagocytosis in the reticuloendothelial system, which is activated and secretes quantities of cytokines. These are presumed that factors exacerbating the disease conditions are hypercytokinemia as well as infection and administration of anti-inflammatory drugs.

REFERENCES

1. Cappellini MD, Fiorelli G. Glucose-6-phosphate dehydrogenase deficiency. *Lancet*. 2008;371:64–74.
2. WHO working group. Glucose-6-phosphate dehydrogenase deficiency. *Bull World Health Organ*. 1989;67:601–611.
3. Hirono A, Fujii H, Hirono K, et al. Molecular abnormality of a Japanese glucose-6-phosphate dehydrogenase variant (G6PD Tokyo) associated with hereditary non-spherocytic hemolytic anemia. *Hum Genet*. 1992;88:347–348.
4. Hirono A, Fujii H, Miwa S. Molecular abnormality of G6PD Konan and G6PD Ube, the most common glucose-6-phosphate dehydrogenase variants in Japan. *Hum Genet*. 1993;91:507–508.
5. Hirono A, Nakayama S, Fujii H, et al. Molecular abnormality of a unique Japanese glucose-6-phosphate dehydrogenase variant (G6PD Kobe) with a greatly increased affinity for galactose-6-phosphate. *Am J Hematol*. 1994;45:185–186.
6. Hirono A, Miwa S, Fujii H, et al. Molecular study of eight Japanese cases of glucose-6-phosphate dehydrogenase deficiency by nonradioisotopic single-strand conformation polymorphism analysis. *Blood*. 1994;83:3363–3368.
7. Hirono A, Fujii H, Takano T, et al. Molecular analysis of eight biochemically unique glucose-6-phosphate dehydrogenase variants found in Japan. *Blood*. 1997;89:4624–4627.
8. Okano Y, Fujimoto A, Miyagi T, et al. Two novel glucose-6-phosphate dehydrogenase variants found in newborn mass-screening for galactosaemia. *Eur J Pediatr*. 2001;160:105–108.
9. Taki M, Hirono A, Kawata M, et al. a new glucose-6-phosphate dehydrogenase variant G&PD Sugao (826C→T) exhibiting chronic hemolytic anemia with episodes of hemolytic crisis immediately after birth. *Int J Hematol*. 2001;74:153–156.
10. Tantular IS, Kawamoto F. An improved, simple screening method for detection of glucose-6-phosphate dehydrogenase deficiency. *Trop Med Int Health*. 2003;8:569–574.
11. Wong CT, Saha N. Haemoglobin, Serum iron, transferrin, ferritin concentrations and total iron-binding capacity in erythrocyte glucose-6-phosphate dehydrogenase deficiency. *Trop Geogr Med*. 1987;39:350–353.
12. Brownell A, Brozovic SM. Serum ferritin concentration in sickle cell crisis. *J Clin Pathol*. 1986; 39:253–255.
13. Damade R, Rosenthal E, Cacoub P. Hyperferritinemia. *Ann Med Interne (Paris)*. 2000;151:169–177.
14. Esumi N, Ikushima S, Hibi S, et al. High serum ferritin level as a marker of malignant histiocytosis and virus-associated hemophagocytic syndrome. *Cancer*. 1988;61:2071–2076.
15. Wei Y, Miller SC, Tsuji Y, et al. Interleukin 1 induces ferritin heavy chain in human muscle cells. *Biochem Biophys Res Commun*. 1990;169:289–296.
16. Feelders RA, Vreugdenhil G, Eggermont AM, et al. Regulation of iron metabolism in the acute-phase response: interferon gamma and tumour necrosis factor alpha induce hypoferraemia, ferritin production and a decrease in circulating transferrin receptors in cancer patients. *Eur J Clin Invest*. 1998;28:520–527.
17. Kanno T, Maekawa M, Kanda S, et al. Evaluation of cytosolic aminopeptidase in human sera. Evaluation in hepatic disorders. *Am J Clin Pathol*. 1984;82:700–705.
18. Pancheva-Haschen R, Haschen RJ. Serum leucine aminopeptidase for monitoring viral infections with plasmacytoid reaction. *Enzyme*. 1986;36:179–186.
19. Sugaya N, Nirasawa M, Mitamura K, et al. Increased cytosol aminopeptidase and lactate dehydrogenase in serum originating from lymphocytes in measles and rubella infection. *Am J Dis Child*. 1988;142:1352–1355.
20. Harris CA, Hunte B, Krauss MR, et al. Induction of leucine aminopeptidase by interferon-gamma. Identification by protein microsequencing after purification by preparative two-dimensional gel electrophoresis. *J Biol Chem*. 1992;267:6865–6869.

A critical role for phagocytosis in resistance to malaria in iron-deficient mice

Chikako Matsuzaki-Moriya[1], Liping Tu[1], Hidekazu Ishida[2], Takashi Imai[2], Kazutomo Suzue[2], Makoto Hirai[2], Kohhei Tetsutani[1], Shinjiro Hamano[1], Chikako Shimokawa[1] and Hajime Hisaeda[2]

[1] Department of Microbiology and Immunology, Graduate School of Medical Sciences, Kyushu University, Fukuoka, Japan
[2] Department of Parasitology, Graduate School of Medicine, Gunma University, Maebashi, Japan

Both iron-deficient anemia (IDA) and malaria remain a threat to children in developing countries. Children with IDA are resistant to malaria, but the reasons for this are unknown. In this study, we addressed the mechanisms underlying the protection against malaria observed in IDA individuals using a rodent malaria parasite, *Plasmodium yoelii* (Py). We showed that the intra-erythrocytic proliferation and amplification of Py parasites were not suppressed in IDA erythrocytes and immune responses specific for Py parasites were not enhanced in IDA mice. We also found that parasitized IDA cells were more susceptible to engulfment by phagocytes in vitro than control cells, resulting in rapid clearance of parasitized cells and that protection of IDA mice from malaria was abrogated by inhibiting phagocytosis. One possible reason for this rapid clearance might be increased exposure of phosphatidylserine at the outer leaflet of parasitized IDA erythrocytes. The results of this study suggest that parasitized IDA erythrocytes are eliminated by phagocytic cells, which sense alterations in the membrane structure of parasitized IDA erythrocytes.

Key words: Iron-deficient anemia · Macrophages · Malaria · Phosphatidylserine

Introduction

Iron deficiency is the most common and widespread nutritional disorder in the world. In many disorders resulting from a lack of iron, hemoglobin synthesis is deeply suppressed, resulting in iron-deficient anemia (IDA). IDA is characterized by small erythrocytes (microcytic) that contain less hemoglobin (hypochromic). IDA is mainly caused by a low dietary intake of iron, but can also be caused by chronic intestinal hemorrhage associated with hookworm infestation or by vitamin A deficiency, which is critical for iron metabolism. Both are common in developing countries [1]. Nearly half of the children living in developing countries are estimated to suffer from IDA; twice the number in industrialized countries. Iron deficiency adversely affects cognitive performance, behavior and physical growth, and IDA patients experience impaired gastrointestinal function and altered patterns of hormone production and metabolism [1]. Moreover, morbidity due to infectious diseases is increased in iron-deficient populations because of its adverse effects on the immune system [1, 2]. Based on this, the World Health Organization recommends iron supplementation for children and pregnant women to treat IDA.

Malaria is still a major health problem, resulting in more than 200 million infections and around a million deaths annually [3]. Almost all victims of malaria are children under 5 years of age living in sub-Saharan Africa [3], whose geographical and age distribution completely overlap those of IDA. Thus, the coexistence of IDA and malaria seems common, and IDA may modulate the course of malaria. In Kenya, however, clinical malaria is significantly less frequent among iron-deficient

Correspondence: Dr. Hajime Hisaeda
e-mail: hisa@med.gunma-u.ac.jp

children [4]. In infants from Papua New Guinea, iron supplementation increased the prevalence of parasitemia [5]. In the largest study, involving Zanzibari children, routine supplementation with iron and folate was found to increase the risk of severe malaria and death [6]. Taken together, these findings suggest that routine supplementation with iron, or iron plus folate, increases childhood morbidity and mortality from malaria. Recently, one study assessed the effect of iron supplementation on the intermittent preventive treatment of malaria [7]; however, the mechanisms involved are still not fully understood.

Here, we addressed the mechanisms underlying decreased susceptibility to malaria in IDA individuals using a mouse malaria model. We found that macrophages preferentially sensed and engulfed parasitized erythrocytes from IDA mice, resulting in rapid clearance of the parasite from the circulation. One possible reason for this rapid clearance may be increased phosphatidylserine (PS) exposure at the outer leaflet of parasitized IDA erythrocytes.

Results

Induction of IDA

C57BL/6 mice were fed with a chemically defined iron-deficient diet to mimic IDA, the most prevalent form of anemia observed in endemic areas of malaria. The effect of this diet on hematopoiesis was assessed by measuring a number of hematological variables (Table 1). Ten weeks of an iron-deficient diet resulted in decreased erythrocyte and hemoglobin concentrations. The MCV (mean corpuscular volume, volume per individual erythrocyte) was also reduced in these mice, confirming the successful induction of IDA characterized by microcytic anemia.

Mice with IDA are protected from early death due to malaria

Iron-deficient mice were infected with *Plasmodium yoelii* (Py) and the kinetics of infection assessed by evaluating the daily levels of parasitemia and survival rates. Py has two substrains, PyL and PyNL, each with differing virulence. Infection of iron-sufficient mice with the virulent strain, PyL, resulted in a rapid increase in parasitemia that killed all mice within 10 days (Fig. 1A). Interestingly, IDA mice showed markedly lower levels of parasitemia throughout the period of infection and survived longer than iron-sufficient control mice. They finally succumbed to infection with low levels of parasitemia, presumably due to severe anemia (Fig. 1A). Mice infected with LD_{50} of the PyNL strain (less virulent than PyL) experienced peak levels of parasitemia 3 wk after infection followed by complete eradication of the parasites. Mice cured of PyNL infection showed sterile immunity against otherwise-lethal infections by PyL [8]. IDA mice had low levels of parasitemia and all of them survived (Fig. 1B). A detailed evaluation showed that the numbers of late trophozoites and shizonts were significantly reduced (Fig. 1C). These results clearly demonstrated that IDA mice were protected from death caused by acute Py infection. This protection was not limited to infection with Py, as similar results were obtained when IDA mice were infected with the *P. berghei* NK65 strain (data not shown).

Table 1. Hematological variables in mice after 10-wk feeding with iron-deficient diet

	Control	ID
Hematocrit (%)	50.0±0.82*	34.3±0.47
Hemoglobin (g/dL)	12.3±0.35*	8.0±0.40
RBC count (10^4/cmm)	911.7±44.97*	731.0±41.70
MCV (fl)	55.0±2.51*	47.1±3.04
MCH (pg)	24.7±0.90	23.2±0.84
MCHC (g/dL)	13.6±1.07	10.93±1.03

Each value represents mean±SD from six mice. Asterisks indicate significant difference between control and ID group. MCV: mean corpuscular volume; MCH: mean corpuscular hemoglobin; MCHC: mean corpuscular hemoglobin concentration.

IDA has no effect on parasite growth

To address the mechanisms underlying resistance to malaria in IDA, two possibilities were raised. One relates to the direct effects on the parasites themselves; the development/growth of the parasites is suppressed in IDA erythrocytes. The other is that iron-deficiency modulates host immunity to enhance the eradication of parasites. We first focused on the intra-erythrocytic development of the malaria parasites. Erythrocytes isolated from IDA mice during the early phase of PyL infection were cultured in the presence of 10% normal mouse serum and periodically observed under a microscope. The purified infected cells were almost ring-infected and developed into late trophozoites within 3 h. They developed into mature schizonts after nuclear division within 6 h. PyL parasites grew equally well in IDA erythrocytes and control erythrocytes (Fig. 2A). To further mimic the in vivo situation, we used serum from IDA mice. Under these conditions the parasites still grew in the presence of IDA serum (Fig. 2A). Furthermore, we did not observe any differences in the number of merozoites within the individual mature schizonts in vivo (Fig. 2B). These results seem to exclude the possibility that IDA adversely affects the development/growth of malaria parasites.

Acquired immunity is not involved in resistance of IDA mice to malaria

We next analyzed the effects of IDA on host immunity. Our previous reports showed that infection with PyL, but not PyNL, activates Tregs, indicating that the virulence of Py is determined by immunosuppression associated with Treg activation [9]. Activation of Tregs during infection with PyL requires TLR9 signaling in DCs

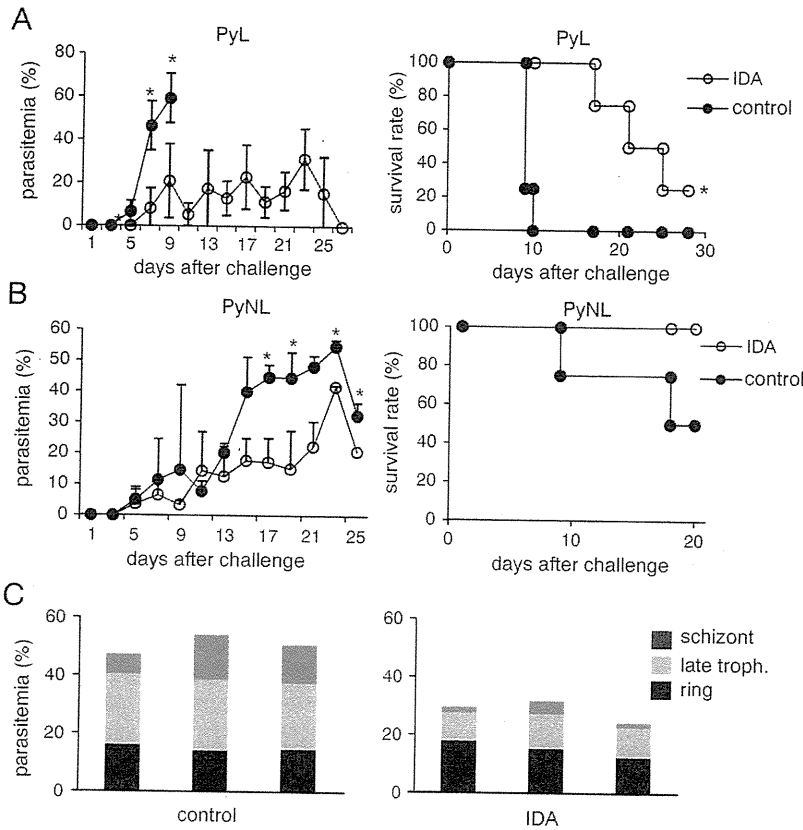

Figure 1. Protection against Py in IDA mice. Percentage parasitemia (left panels) and survival rates (right panels) in mice infected with (A) PyL or (B) PyNL. Data are presented as the mean parasitemia ± SD (from six mice). In the left panels, asterisks represent significant differences ($p<0.05$) in parasitemia (%) between IDA and control mice. In the right panels, asterisks indicate statistical significance ($p<0.05$) using the Breslow-Gehan-Wilcon test of the Kaplan–Meier method between IDA and control mice. (C) Parasitemia during each erythrocytic stage in mice infected with PyL. The results from three individual mice obtained 6 days after infection are shown. Four repeated experiments showed similar results.

[10]. It is quite possible that Tregs are not activated in IDA mice due to insufficient TLR9 signaling because IDA erythrocytes contain much less hemoglobin/heme (data not shown), the source of a known malaria-derived TLR9 ligand, hemozoin [11]. Thus, we analyzed the immune responses in IDA mice. First, we assessed the number of cells involved in protection against malaria in the spleen 6 days after infection with PyL (Fig. 3A). Infection with PyL clearly increased the population of spleen cells. Unexpectedly, the number of whole splenocytes and splenic $CD4^+CD25^-$ T cells in IDA mice was less than that in control mice. There was no increase in the number of macrophages.

IFN-γ production by whole spleen cells in response to ConA was evaluated using ELISA. Infection of control mice with PyL markedly reduced the production of IFN-γ; however, infection of IDA mice reduced it to an even greater degree (Fig. 3B). The production of IgG antibodies specific for the malaria parasite was also assessed. Humoral immunity to the malaria parasite was induced after infection with PyL in iron-sufficient mice. However, IDA mice had much lower total IgG levels (Fig. 3C). Thus, neither humoral nor cellular responses were enhanced in IDA mice.

We further evaluated the functional properties of splenic Tregs by investigating the suppression of TCR-driven T-cell proliferation. $CD4^+CD25^+$ T cells isolated from IDA mice were cultured with $CD4^+CD25^-$ T cells from uninfected mice in the presence of ConA. Tregs from uninfected mice suppressed proliferation in a dose-dependent manner. Infection of iron-sufficient mice with PyL markedly enhanced the suppressive function of Tregs, reflecting Treg activation (Fig. 3D). Tregs in IDA mice had much stronger suppressive abilities (Fig. 3D), presumably resulting in reduced immune responses in these mice. Again, we saw no evidence for the enhancement of acquired immunity in IDA mice.

Finally, to analyze whether acquired immunity is involved in the resistance of IDA mice to malaria, we infected T-cell and iron-deficient athymic nude mice with PyL. As shown previously, IDA euthymic mice showed lower levels of parasitemia and prolonged survival compared with euthymic mice fed with an iron-sufficient diet (Fig. 3E). IDA athymic mice clearly showed lower levels of parasitemia than mice fed with an iron-sufficient diet although they still succumbed to infection with PyL. These results suggest that acquired immunity, in which T cells play a central role, is required to survive infection by PyL, but it is not involved in IDA-associated resistance to malaria during the early phase of infection.

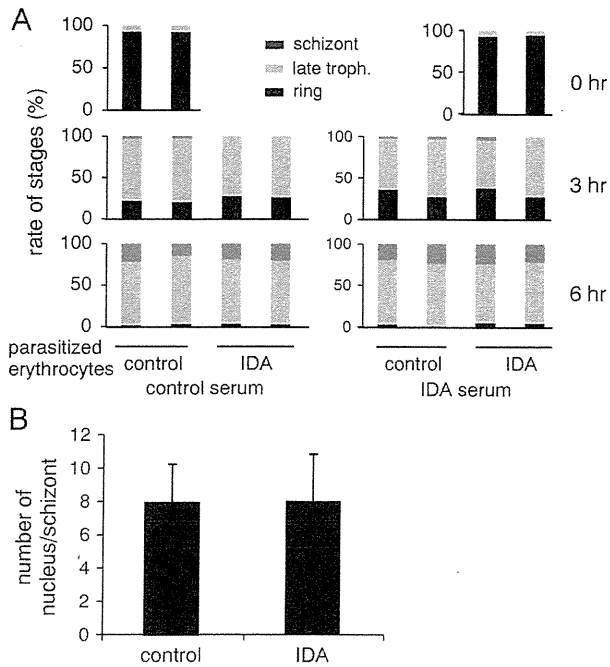

Figure 2. Intra-erythrocytic development and amplification of PyL in IDA erythrocytes. (A) Erythrocytes infected with the ring form of PyL from IDA mice were cultured in the presence control serum (left panels) or serum from IDA mice (left panels) and the developmental stages assessed microscopically after the indicated culture periods. The ratio of erythrocytes infected with ring form, late trophozoite, and schizonts to the total number of erythrocytes infected with asexual parasites is shown. Three individual mice were used in each group. (B) The number of merozoites in schizont-infected erythrocytes in whole blood obtained from IDA mice was counted under a microscope. Blood smears were prepared on 7, 9, and 11 days after challenge. Data represent the means ± SD from 150 schizonts. Three repeated experiments showed similar results.

Enhanced phagocytosis of IDA erythrocytes infected with Py

Considering the resistance observed in IDA mice during the very early phase of infection, innate immunity and/or more primitive protective mechanisms might be operating. One of the first lines of defense against blood-stage malaria is phagocytosis followed by digestion of parasitized erythrocytes by phagocytic cells [12]. To examine the possibility that the phagocytic ability of macrophages is involved in resistance, peritoneal macrophages obtained from IDA mice were cultured with CFSE-labeled parasitized erythrocytes purified from PyL-infected iron-sufficient mice and analyzed for their phagocytic ability. Macrophages from both iron-sufficient and iron-deficient mice phagocytosed parasitized erythrocytes, but not uninfected erythrocytes (Fig. 4A). Activation of phagocytes in IDA mice could not explain this phenomenon.

Previous reports showed that parasitized IDA erythrocytes are engulfed by phagocytic cells [13]. Therefore, we assessed the difference in susceptibility to phagocytosis between IDA and control parasitized erythrocytes. Percoll-purified schizonts from IDA mice infected with PyL were labeled with CFSE and cultured with peritoneal macrophages obtained from control mice. As shown previously, a small population of $CD11b^+$ macrophages ingested parasitized erythrocytes from iron-sufficient mice (Fig. 4B). Surprisingly, almost all macrophages phagocytosed parasitized IDA erythrocytes. $CD11b^+$ macrophages contained higher levels of CFSE, suggesting engulfment of multiple parasitized erythrocytes (Fig. 4B). This enhanced susceptibility to phagocytosis was limited to parasitized cells, as macrophages did not ingest erythrocytes from uninfected IDA mice (Fig. 4B). Similar results were obtained using macrophages isolated from the spleen, in which the malarial parasites encounter host immune cells (Fig. 4C). To further analyze these observations in vivo, we intravenously inoculated uninfected mice with CFSE-labeled parasitized IDA erythrocytes and examined their clearance from the circulation. Uninfected erythrocytes were constantly detected throughout the entire course of the experiment (Fig. 4D). Consistent with the in vitro studies, purified schizonts from IDA mice were more rapidly eliminated from the circulation than those from control mice (Fig. 4D). This was more obvious when purified ring-infected erythrocytes were used. The clearance of ring-infected erythrocytes from IDA mice was comparable to that of schizonts, whereas ring-infected iron-sufficient erythrocytes were retained for up to 60 min (Fig. 4D). $F4/80^+$ red pulp macrophages may be responsible for phagocytosis of IDA parasitized erythrocytes in vivo (Fig. 4E).

The rapid clearance of parasitized IDA erythrocytes is due to the enhanced ability of phagocytic cells to capture them. Mice treated with carrageenan (CGN), which impairs the function of phagocytic cells, showed a significant delay in the elimination of IDA schizonts. In contrast, iron-sufficient schizonts were eliminated regardless of whether they were treated with CGN (Fig. 5A). Finally, we evaluated the contribution of enhanced phagocytosis of parasitized IDA erythrocytes to the resistance of IDA mice to malaria. Treatment with CGN completely reversed the lower levels of parasitemia and prolonged survival of IDA mice infected with PyL, but did not alter the course of infection in iron-sufficient mice (Fig. 5B). These results indicate that phagocytosis of parasitized IDA cells plays a critical role in resistance to malaria in IDA mice.

PS exposure in IDA parasitized erythrocytes

We next explored the mechanisms underlying the enhanced phagocytosis specific for parasitized IDA erythrocytes by focusing on alterations in the membrane structure, especially the increased exposure of PS, which is usually located within the inner leaflet of the lipid bilayer. Exposure of PS is one of the hallmarks of apoptotic nucleated cells and provides an "eat me" signal to phagocytic cells, resulting in rapid clearance of apoptotic cells without any inflammatory consequences. PS-dependent phagocytosis is involved in the physiological clearance of erythrocytes after their natural lifespan [14]; therefore, we estimated the levels of PS exposure in IDA mice

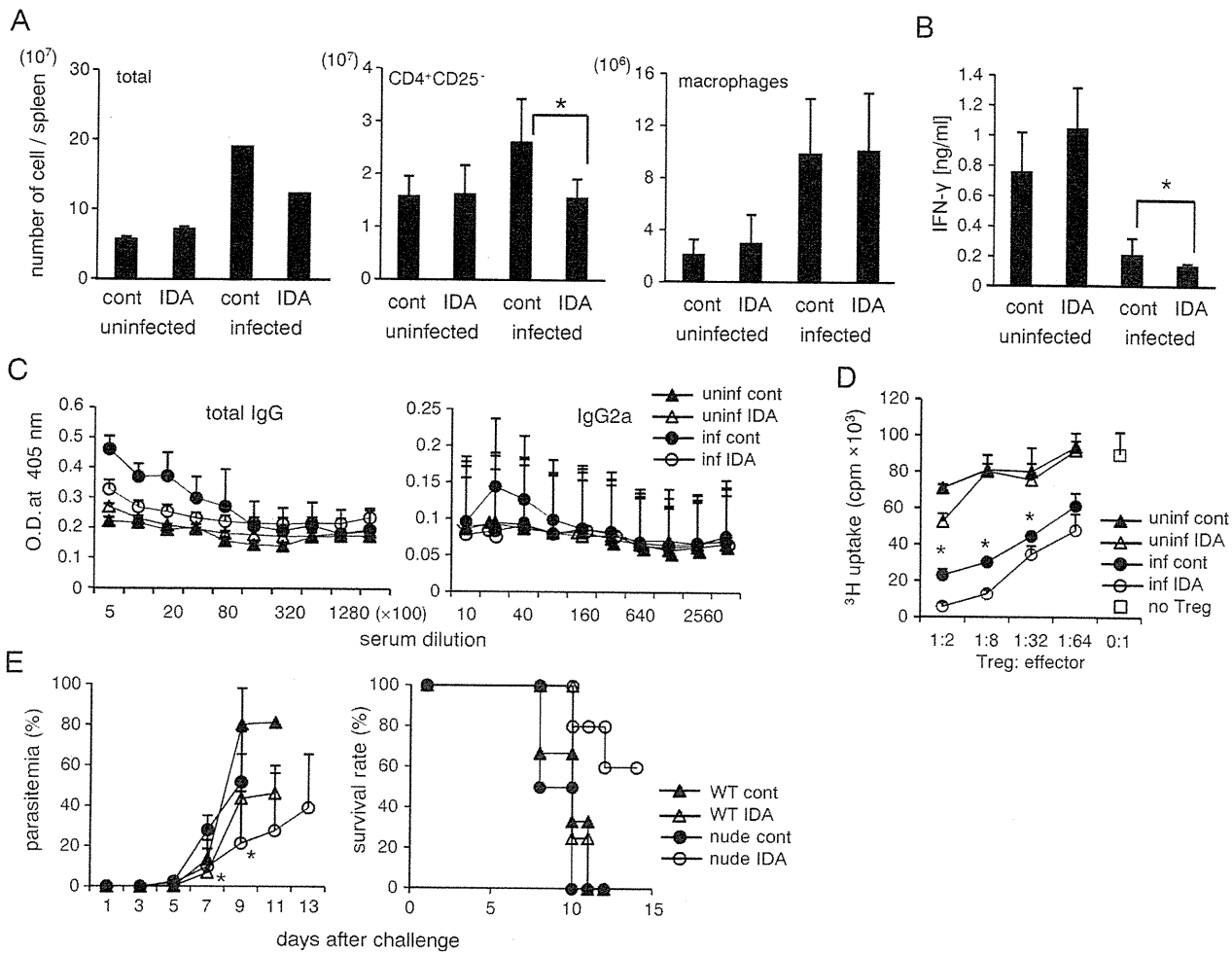

Figure 3. Effects of IDA on acquired immunity in mice infected with Py. Spleen cells obtained 6 days after infection by PyL were analyzed for (A) the number of the indicated cells and for (B) IFN-γ production after 48 h of culture with ConA. Data represent the mean ± SD from 6 mice (A) or 3 mice (B). *$p<0.05$. (C) Sera were obtained from the indicated mice 7 days after infection. Antibodies specific for parasite antigens were analyzed by ELISA. The vertical and horizontal axes represent OD at 405 nm and the dilution factor, respectively. Results represent the mean ± SD of triplicate wells. Each group contained three mice. (D) To examine the suppressive function of $CD4^+CD25^+$ cells after PyL infection, $CD4^+CD25^-$ T cells (2×10^5) purified from uninfected mice were stimulated with ConA and APC in the presence of $CD25^+$ T cells from uninfected controls (filled triangles), uninfected IDA (open triangles), infected controls (filled circles) and infected IDA (open circles) mice 5 days after infection at the indicated ratio to $CD4^+CD25^-$ T cells. Asterisks denote significant differences ($p<0.05$) in ^{3}[H]-thymidine uptake (cpm) between infected controls and infected IDA groups. (E) To assess the effects of IDA on susceptibility of T-cell-deficient nude mice, we infected the indicated mice with PyL and monitored parasitemia and survival rate. Values for parasitemia are arithmetic means ± SD from six mice in each group. *$p<0.05$, in parasitemia between iron-sufficient and IDA WT mice and between iron-sufficient and IDA nude mice 7 and 9 days after infection, respectively (left panel). Two repeated experiments showed similar results.

infected by PyL using flow cytometry to analyze the binding of annexin V. Peripheral blood was stained with an anti-CD71 (transferrin receptor) antibody and Syto 16, which binds to nucleic acids, to distinguish parasitized erythrocytes from reticulocytes, which are increased in IDA mice. Syto 16 stained both parasite-derived nucleic acids and the residual RNA in reticulocytes. Because PyL invades mature erythrocytes – but not reticulocytes – expressing CD71 [15], Syto 16^+ cells within the $CD71^-$ mature erythrocytes represented parasitized erythrocytes. The percentage of annexin V-binding parasitized erythrocytes in the IDA mice was markedly increased compared with that in the control mice (Fig. 6), suggesting that increased exposure of PS resulted in higher susceptibility of IDA erythrocytes to phagocytosis. It should be noted that a substantial fraction of uninfected erythrocytes bound annexin V, suggesting that infection may have an effect on membrane remodeling in uninfected as well as in infected cells.

Cytosolic Ca^{2+} concentration increases in IDA erythrocytes after infection with PyL

Finally, we analyzed the putative mechanisms underlying PS exposure in parasitized IDA erythrocytes. The enzymes

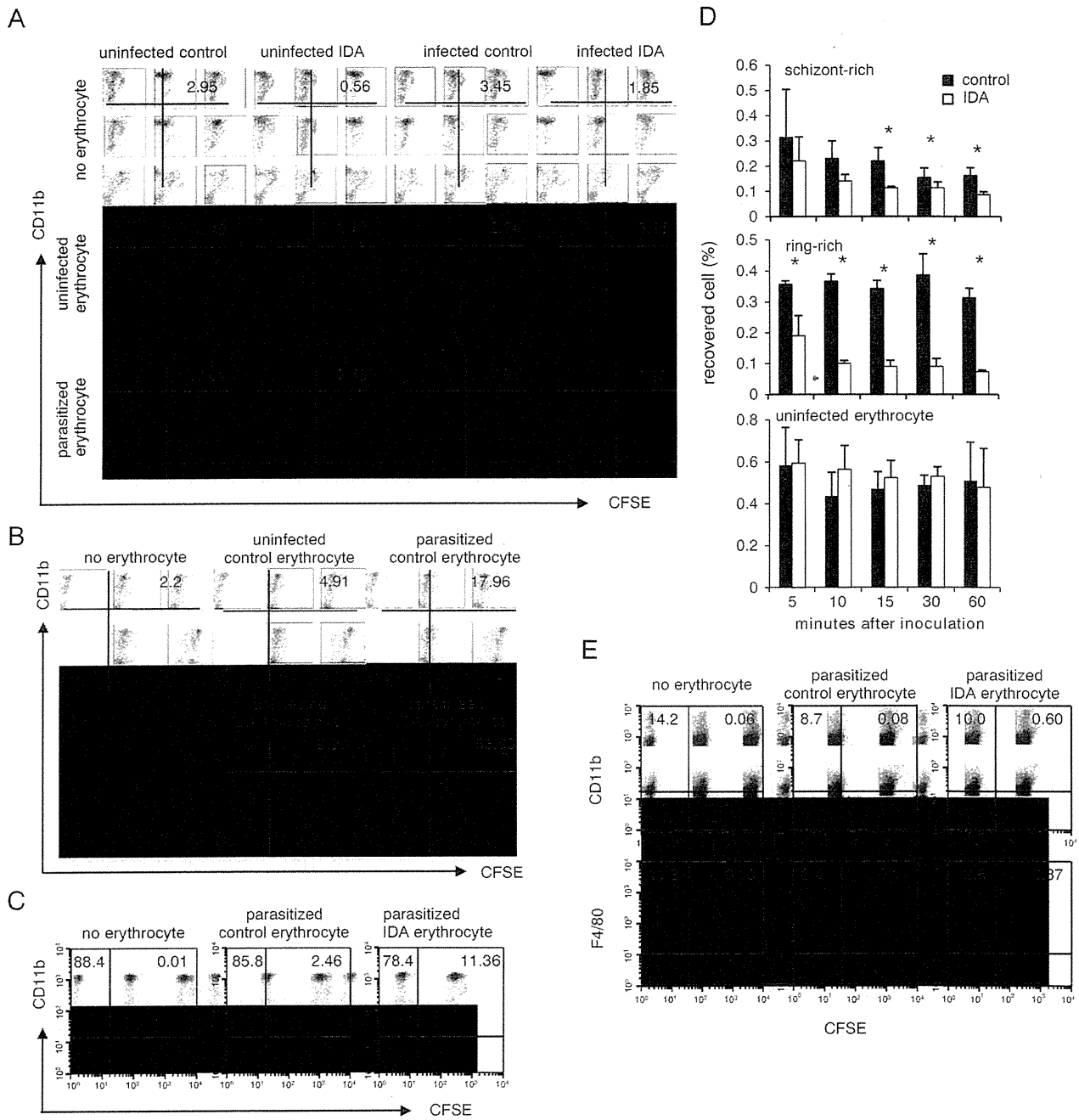

Figure 4. Rapid clearance of IDA erythrocytes infected with malaria parasites. (A) Macrophages isolated from the indicated mice were cultured with CFSE-labeled parasitized erythrocytes (bottom panels) obtained from iron-sufficient mice infected with PyL. Two hours later, macrophages were analyzed for their capacity to ingest erythrocytes using flow cytometry. The numbers represent the mean percentages of $CD11b^+$ macrophage-engulfed erythrocytes from three individual experiments. (B) Peritoneal and (C) splenic macrophages isolated from iron-sufficient, uninfected mice were cultured with CFSE-labeled erythrocytes isolated from the indicated mice. Phagocytosis was assessed as above. All experiments were performed in triplicate. (D) Mice were transfused with CFSE-labeled schizont-infected erythrocytes (top panel) or with schizont-free erythrocytes (middle panel) isolated from control (filled columns) and IDA mice infected with PyL (open columns). Mice were given erythrocytes from uninfected recipients (bottom panel). Peripheral blood was collected and analyzed for $CFSE^+$ cells using flow cytometry at the indicated time points after inoculation. Values represent means ± SD ($n = 3$) of the percentage of the transfused erythrocytes within the whole erythrocyte population in the circulation. Asterisks indicate significant differences between IDA and control erythrocytes. (E) Splenic macrophages, isolated from mice injected with the indicated cells labeled with CFSE, were analyzed for phagocytosis in vivo 90 min after injection. Data represent the mean ($n = 3$) of the percentages within each quadrant. Two repeated experiments showed similar results.

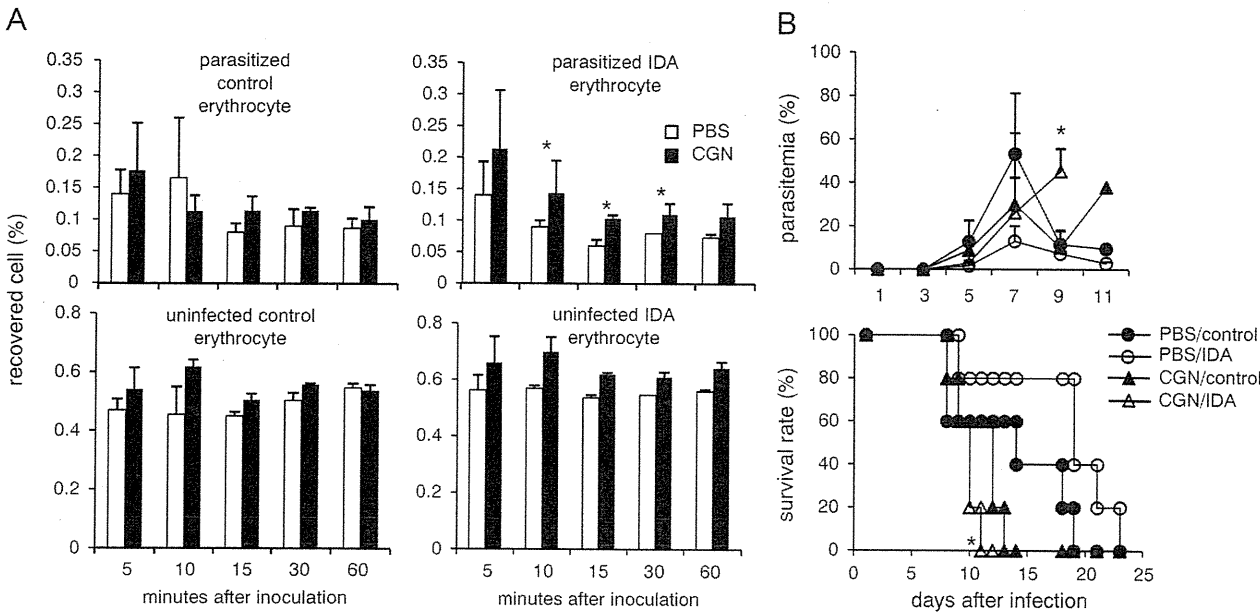

Figure 5. Reversal of resistance to Py by inhibiting macrophage phagocytosis. (A) Mice treated with (filled columns) or without CGN (open columns) were inoculated with uninfected (bottom) or infected erythrocytes (upper) isolated from iron-sufficient (left panels) or IDA mice (right panels). Transfused cells were analyzed as in Fig. 4D. (B) To evaluate the effects of blocking phagocytosis on the resistance to malaria, control (filled symbols) and IDA mice (open symbols) treated with (triangles) or without (circles) CGN were infected with PyL. Parasitemia and survival rate were monitored. Values for parasitemia are arithmetic means ± SD from six mice in each group. Asterisks indicate significant differences in parasitemia (upper panel) or in survival (lower panel) between IDA mice treated with or without CGN. Two repeated experiments showed similar results.

responsible for the changing the composition between the outer and inner leaflets of the plasma membrane lipid bilayer are scramblase, flippase and floppase (aminophospholipid translocase (APT)). Scramblase, located under the inner monolayer, carries inner phospholipids to the outer monolayer following an increase in cytosolic Ca^{2+} concentration. Some studies report that erythrocytes infected with malaria parasites show substantial increases in Ca^{2+} concentration [16], which led us to examine the Ca^{2+} concentration in IDA erythrocytes. As shown in Fig. 7, fluorescence microscopic analyses of erythrocytes stained with the Ca^{2+} indicator, Flou-4/AM, revealed a marked accumulation of Ca^{2+} in the cytosolic spaces within parasitized IDA erythrocytes, whereas those from iron-sufficient mice showed limited increases in Ca^{2+} associated with the nuclei (parasites).

Discussion

Iron deficiency, leading to a typical microcytic hypochromic anemia, is a widespread and common nutritional problem in developing countries. Many people suffer from IDA in areas that are endemic for malaria [2], and it is known that IDA individuals are protected against malaria. Because IDA influences sporozoite development in the liver [17], it is possible that the severity of the blood-stage infection might be modified in humans due to alterations during the earlier stages; however, in this study, we found that IDA mice were highly resistant to erythrocytic-stage

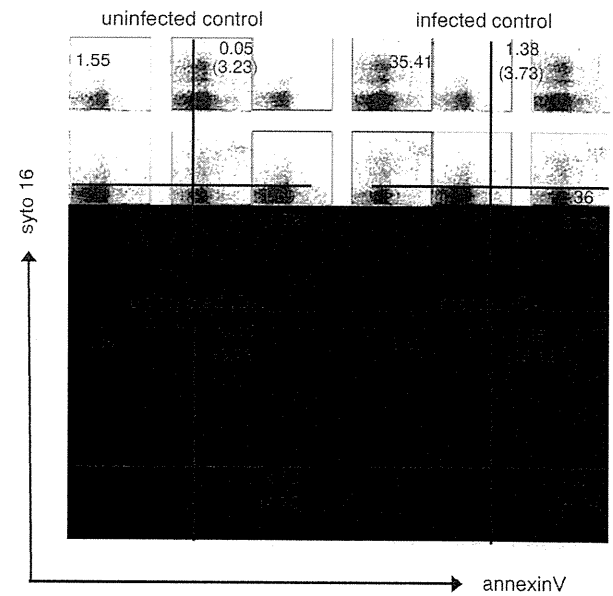

Figure 6. Increased phosphatidylserine exposure in IDA erythrocytes infected with Py. Gated TER119$^+$CD71$^-$ erythrocytes from IDA or control mice infected with PyL were stained 9 days after infection with annexin V and Syto 16. The numbers indicate the mean ratios within each quadrant. Numbers in parentheses indicate ratio of annexin V binding cells to parasitized (upper right) or uninfected erythrocytes (lower right) from three mice. The ratio of annexin V$^+$ cell:parasitized cells in IDA mice (asterisk) was significantly higher than that in control mice. Three repeated experiments showed similar results.

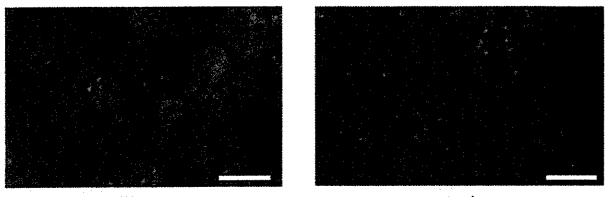

Figure 7. Evaluation of intracellular Ca^{2+} concentrations in erythrocytes from IDA mice. Erythrocytes from IDA or control mice infected with PyL were obtained and analyzed. Intracellular Ca^{2+} was visualized using Fuol-4/AM dye (green) under a fluorescence microscope. Parasite nuclei were stained with Hoechst stain (blue). Scale bars indicate 10 μm (original magnification: ×600). Three repeated experiments showed similar results.

malaria, and we addressed the mechanisms underlying resistance to malaria in IDA.

First, we analyzed whether IDA affects the intra-erythrocytic development of the parasites. PyL parasites grew and proliferated in IDA erythrocytes in a manner comparable with that in control erythrocytes, even when cultured in the presence of low levels of iron (Fig. 2A). The resulting schizont-infected IDA erythrocytes contained similar numbers of intracellular merozoites to those in control erythrocytes (Fig. 2B). An alternative possibility is that IDA erythrocytes are more resistant to parasite invasion. Although we could not test this because of technical limitations in the use of murine parasites [18], it is unlikely, as Luzzi et al. proved, that *P. falciparum* invades IDA erythrocytes to the same degree as control erythrocytes [19]. Thus, we speculated that IDA does not adversely affect the parasites themselves and that resistance in IDA might be associated with host protective mechanisms.

In addition to the lower levels of parasitemia during the very early phase of infection, acquired immunity is not well developed, suggesting that primitive protective mechanisms may operate. Indeed, we found that parasitized IDA cells were more susceptible to engulfment by phagocytes than control cells in vitro, resulting in rapid clearance from the circulation (Fig. 4). Furthermore, inhibition of phagocytosis slowed the clearance of parasitized IDA cells and abrogated resistance to infection by PyL in IDA mice (Fig. 5), demonstrating that the resistance observed in IDA mice was mainly dependent on phagocytosis. Our findings also showed that phagocytosis of ring-stage parasites, prior to the development of parasites capable of sequestration (Fig. 1C, Fig. 4D), may account for the reduced incidence of severe malaria in IDA patients. It would be interesting to investigate this using a model of experimental cerebral malaria.

We speculated that the higher susceptibility of IDA erythrocytes to phagocytosis results from the exposure of PS during parasite development, although we could not prove this experimentally. As apoptotic nucleated cells are phagocytosed after recognition by macrophages expressing receptors specific for PS [20], erythrocytes with exposed PS might be taken up by these macrophages. Several conditions, including aging, induce PS exposure in erythrocytes resulting in their rapid clearance [14]. Iron-deficiency may also increase PS exposure. One possible mechanism is that IDA erythrocytes have reduced levels of glutathione peroxidase, leading to higher sensitivity to oxidative stress, a major cause of PS externalization by erythrocytes [21]. Oxidative stress also induces alterations in band 3 in erythrocytes, resulting in them being recognized and phagocytosed by macrophages in a PS-independent manner [22].

Another possibility is that the enzymes involved in PS exposure are altered in IDA. Externalization of PS is regulated by three enzymes: a Ca^{2+}-dependent scramblase, which catalyzes the bidirectional movement of phospholipids across the lipid bilayer; an ATP-dependent APT, which mediates the energy-dependent transfer of phospholipids from the outer to the inner leaflet; and a third enzyme that mediates the energy-dependent transfer of phospholipids from the inner to the outer leaflet [23]. It is reported that activation of scramblase and dysfunction of APT are responsible for PS exposure in erythrocytes [24, 25]. We observed that cytosolic Ca^{2+} concentrations increased in parasitized IDA erythrocytes, which may indicate scramblase activation. Measuring ATP concentrations would be interesting to deduce the activity of APT. Increases in Ca^{2+} concentration also activate calpain, a protease that degrades spectrin [26], which might affect the structure and the susceptibility of erythrocytes to phagocytosis.

As previously reported [2, 4], we found that T-cell responses in IDA mice were decreased (Fig. 3A–C). In general, iron-deficiency results in impaired immunity, mainly because the enzymes regulating immune responses and DNA replication require iron [27]. In addition to the lack of iron, activation of Tregs may participate in downregulation of T-cell-mediated immunity. Tregs from IDA mice showed enhanced suppressive functions (Fig. 3D) presumably related to PS-mediated phagocytosis of parasitized IDA erythrocytes. Because PS receptors are responsible for the downregulation of inflammatory responses after uptake of apoptotic cells [20], activation of Tregs might be one of the immunosuppressive consequences of PS-mediated phagocytosis. Indeed, an immunosuppressive cytokine crucial for Treg function, TGF-β, is vigorously produced during phagocytosis of apoptotic cells [20]. Furthermore, Kleinclauss et al. reported that Tregs are involved in the protective effects seen after apoptotic cell administration in graft-versus-host disease [28]. Thus, it is quite possible that parasitized IDA erythrocytes with exposed PS have immunomodulatory characteristics.

In conclusion, parasitized IDA erythrocytes tend to be eliminated by phagocytic cells that sense alterations in the membrane structure of parasitized erythrocytes. Resistance to malaria in patients with hemoglobin variants is partially explained by the higher susceptibility of mutant erythrocytes to phagocytosis [29–31]. Here, we provide the first in vivo evidence that phagocytosis of parasitized erythrocytes is critical for resistance to malaria in IDA mice. Evaluation of whether this is the case in humans is important for the development efficient therapeutic strategies for both malaria and IDA.

Materials and methods

Mice and parasites

Animal experiments were performed according to the guidelines for animal experimentation of Kyushu University. C57BL/6 mice (female, aged 5 wk) were obtained from Kyudo (Tosu, Japan) and BALB/c nu/nu (nude) mice from CLEA (Japan). IDA mice were bred as described elsewhere [32]. Briefly, C57BL/6 mice, or nude mice, were fed either a control or iron-deficient diet for 10 wk. The diet contained 33% cornstarch, 22% casein, 5% cellulose powder, 30% sucrose, 5% corn oil, 1% AIN-76 vitamin mixture containing 20% choline chloride, 0.02% *p*-aminobenzoic acid, and 4% Harper's mineral mixture without ferric citrate. Ferric citrate, providing 180 mg of iron per kg of final diet, was added to the control diet. Iron-deficient diets contained <10 mg/kg of iron. Mice were housed in plastic cages fitted with stainless steel mesh bottoms to prevent them from ingesting feces.

Blood-stage parasites of *P. yoelii* 17XL (PyL) and *P. yoelii* 17XNL (PyNL) were used in all the experiments (original source: Middlesex Hospital Medical School, University of London 1984). Those two strains have differing virulence, primarily caused by differences in their host cell preference. PyL preferentially invades mature erythrocytes, whereas PyNL mainly infects reticulocytes [15]. Mice were infected intraperitoneally with 25 000 Py-infected erythrocytes obtained from mice freshly inoculated with a frozen stock of the parasites. Parasitemia was checked by Giemsa staining every 2 days and represented as the percentage of parasitized erythrocytes within the total number of erythrocytes.

Hematological analysis

Whole blood was drawn from anesthetized mice by retro-orbital venipuncture. The hemoglobin concentration was measured on the day before challenge by the cyanmethemoglobin method using Drabkin's Reagent (Sigma, St. Louis, MO, USA) according to the manufacturer's instructions [33].

Separation of parasitized erythrocytes

Parasitized erythrocytes were prepared as previously described [34]. Briefly, blood from Py-infected mice was collected with heparin, and passed through a cellulose column to remove WBCs. The RBC solution was placed onto 55% v/v Percoll (Sigma)/PBS and centrifuged and the parasitized erythrocytes at the interface were collected. The purity of the schizonts was usually $>95\%$. The pellets containing ring-infected and uninfected erythrocytes were used as ring stage erythrocytes. In some experiments, parasitized erythrocytes were stained with CSFE (Molecular Probes, Eugene, OR, USA) at 1 μM or 5 μM in PBS) for 20 min at 37°C followed by extensive washing.

In vitro *Plasmodium yoelii* culture

In vitro culture of Py was started at 3% hematocrit, 1–5% parasitized erythrocytes/total RBC, in PRMI-1640 supplemented with 100 IU/mL penicillin, 100 μg/mL streptomycin, 2 mM L-glutamine and 10% inactivated mouse serum. Incubation was carried out under mixed gas consisting of 90% N_2, 5% O_2 and 5% CO_2 at 37°C for 12 h.

ELISA for anti-malaria Abs

Serum from each animal was assayed. Antibodies recognizing Py extracts coated onto Maxisorb plates (Nunc, Roskilde, Denmark) were detected using HRP-conjugated goat anti-mouse IgG or IgG2a, (Zymed Laboratories, San Francisco, CA, USA). Serum samples were run in triplicate and absorbance was read at 405 nm.

Interferon (IFN)-γ ELISA

IFN-γ concentrations were measured in the supernatants from 5×10^5 whole spleen cells 48 h after stimulation with 2 μg/mL of Con A using the mouse IFN-γ Development Kit, Duo Set (R&D Systems, Minneapolis, MN, USA) according to the manufacturer's instructions.

Cell purification and culture

Cell purification was performed using a magnetic cell sorting system (MACS) according to the manufacturer's instructions (Miltenyi Biotech, Bergisch Gladbach, Germany). Mouse spleens were prepared as single cell suspensions. To purify $CD4^+CD25^+$ T cells, the suspensions were incubated with phycoerythrin (PE)-anti-CD25 antibodies (eBioscience, San Diego, CA, USA) followed by anti-PE microbeads (Miltenyi Biotec). $CD4^+CD25^+$ cells were positively selected and used as Tregs. The flow-through cells were incubated with fluorescein isothiocyanate (FITC)-anti-CD4 (eBioscience) followed by anti-FITC microbeads, (Miltenyi Biotec) to yield $CD4^+CD25^-$ T cells. The purity of each cell subset was routinely $>80\%$. Purified $CD4^+$ $CD25^+$ T cells and naïve $CD4^+$ $CD25^-$ T cells were stimulated with Con A at a concentration of 2.5 mg/mL in the presence of APC in 0.2 mL of media (for 72 h) and incubated with 1 Ci/well of $[^3H]$ thymidine for the final 8 h. Radioactivity was measured in a liquid scintillation counter.

Flow cytometry

Single-cell suspensions stained with fluorescence-labeled antibodies were analyzed using a FACSCalibur flow cytometer